Desalination and Water Treatment
www.deswater.com

doi: 10.1080/19443994.2014.886299

54 (2015) 707–714
April

Taylor & Francis
Taylor & Francis Group

Thermodynamics and kinetics of adsorption of a cationic dye onto sepiolite

Özkan Demirbaş*, Yasemin Turhan, Mahir Alkan

Faculty of Science and Literature, Department of Chemistry, University of Balikesir, Balikesir 10145, Turkey
Tel. +90 2666121000; Fax: +90 2666121015; email: ozkan@balikesir.edu.tr

Received 22 November 2013; Accepted 16 January 2014

ABSTRACT

The adsorption kinetics and thermodynamics of Maxilon Red GRL (MR-GRL), a cationic textile dye, onto sepiolite were investigated in aqueous solution in a batch system. The effect of contact time, stirring speed, initial dye concentration, initial solution pH, ionic strength, and temperature was studied. The initial tested concentrations of MR-GRL solution were 1.5×10^{-3}, 2.0×10^{-3} and 2.5×10^{-3} mol/L. The effect of pH was analyzed in the pH range from 5 to 10. The effect of ionic strength was investigated at 0.001–0.100 mol/L NaCl salt concentrations. The experiments were carried out at 288, 298, 308, and 318 K set with a thermostat. The all parameters significantly influenced the adsorption rate and capacity. Experimental data were fitted to pseudo-first order, second-order, Elovich equation, mass transfer, and intra-particle diffusion models. The adsorption kinetics data showed that this process can be described by the pseudo-second-order model, from which the rate constant and the adsorption capacity were determined. The thermodynamic activation parameters such as the activation energy, enthalpy, entropy, and Gibbs free energy were determined. The value of the standard enthalpy change (19.92 kJ/mol) indicates that the adsorption is physical in nature involving weak forces of attraction and is also endothermic. The results showed the applicability of this clay as an efficient adsorbent for cationic dyes.

Keywords: Adsorption; Kinetics; Wastewater; Maxilon Red GRL; Thermodynamics

---

1. Introduction

Various kinds of synthetic dyestuffs appear in the effluents of wastewater in some industries such as dyestuff, textiles, leather, paper, and plastics. [1]. Discharge of dye-bearing wastewater into natural streams and rivers from textile, paper, carpet, leather, distillery, and printing industries poses severe problems because dyes impart toxicity to the aquatic life [2]. The presence of very small amounts of dyes in water is highly visible and undesirable to use [3]. Many techniques have been used for removal of dye-containing wastewater such as chemical oxidation, membrane filtration, biodegradation, separation and adsorption techniques [4]. The kinetics of adsorption and sorption in a complex porous media has been an important subject at the processes of separation and purification. Kinetics and velocity are in the course of investigation of adsorption mechanism. Prediction of the rate of adsorption for a given system is probably the most important factor in adsorption system design. While applying the process, the presence of diffusion and mass transfer coefficient is an important parameter [5–8].

---

*Corresponding author.

Many workers find alternative sorbents particularly for the sorption of basic and acidic dyes, such as activated carbon, unburned carbon [4,9], silica, montmorillonite [10,11], and natural adsorbents such as hen feather [12–15], de-oiled soya [16,17], eggshell [18], eggshell membrane [19], eggshell powder [20], ash [21], peanut husk [22–24], and coconut-husk [25], which have been extensively used as adsorbents.

Sepiolite is an oxide mineral with a unit cell formula $Si_{12}O_{30}Mg_8(OH,F)_4(H_2O)_4.8H_2O$ [26]. In some aspects, sepiolite is similar to other 2:1 trioctahedral silicates, such as talc, molecule formula is $Mg_3Si_4O_{10}(OH)_2$ [26,27]. Sepiolites, which form an important group of clay minerals, are a magnesium silicate and currently used in a number of different applications such as many industrial, catalytic, and environmental process most of which are similar to those of the more traditional clays. The computer-generated model of the sepiolite lattice has been given in Fig. 1, which arranged with some modifications from Refs. [27,28].

The aim of this study was to determine the adsorption kinetics of cationic Maxilon Red GRL (MR-GRL) on sepiolite over a range of physicochemical conditions. These conditions are important to identify various natural environmental systems. For a successful process, kinetic studies are essential since they describe the adsorbate removal rate, which in turn controls the residence time in the adsorbent–solution interface. A number of experimental parameters in this study were considered, including the effect of stirring speed, initial dye concentration, initial solution pH, ionic strength, and solution temperatures. The thermodynamic activation parameters of the process, such as activation energy, enthalpy, entropy, and the free energy, are also determined.

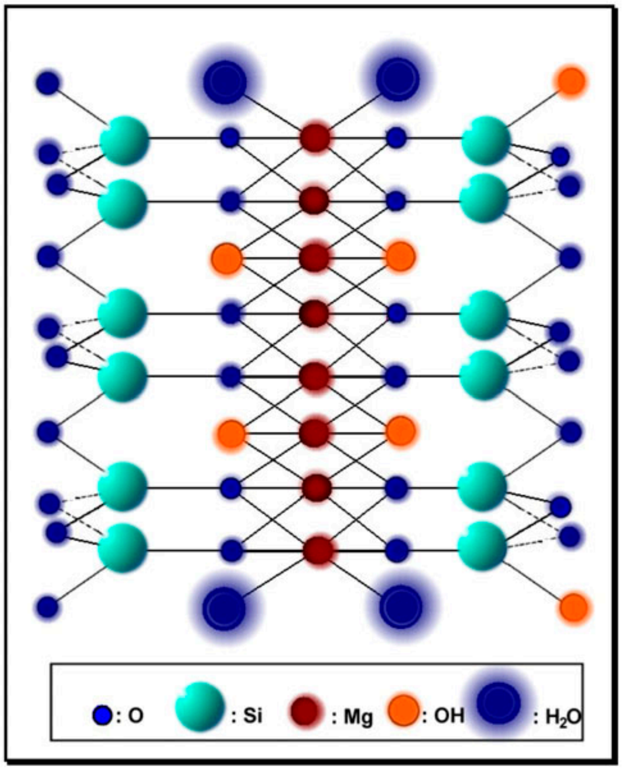

Fig. 1. Computer generated model of the sepiolite lattice.

2. Materials and methods

2.1. Dye

MR-GRL was obtained from Setas and Eksoy Textile Co. (Bursa, Turkey). The molecular structure of MR-GRL used is shown in Fig. 2.

2.2. Sepiolite

The sepiolite used was obtained from Aktaş¸ Lületaşı–Eskişehir regions of Anatolia (Turkey). Sepiolite sample was treated before using in the experiments as follows [29]:

The aqueous suspension was mechanically stirred for 24 h, after the supernatant suspension was filtered through filter paper to separate the sepiolite. The solid sample was dried at 105˚C for 24 h, then ground sieved. The chemical composition of this clay obtained by X-ray florescence is given in Table 1.

The cation exchange capacity (CEC) of the sepiolite used was determined by ammonium acetate method, the density and the specific surface area were measured BET N_2 adsorption by Micromeritics Flow Sorb II-2300 equipment and the other physicochemical parameters, obtained are summarized in Table 2.

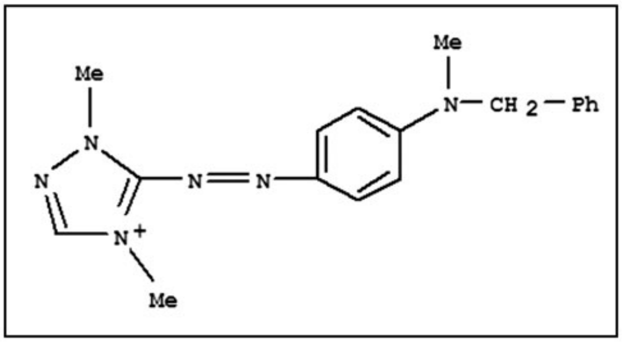

Fig. 2. Structures of MR-GRL.

Table 1
Chemical composition of sepiolite

Constituent	Percentage present
SiO_2	55.60
MgO	22.33
Al_2O_3	0.81
NiO	0.40
CaO	0.22
Fe_2O_3	0.50
Na_2O	0.11
K_2O	0.17
LoI (Loss of ignition)	16.86

X-ray measurements were performed using a Philips X-ray diffractometer employing nickel-filtered Cu*Kα* radiation. X-ray diffraction pattern of sepiolite is given in Fig. 3. Scans were performed over the 2*θ* range from 5˚ to 70˚. The XRD study (Fig. 3) shows that the main phase constituent of the raw material (S) is a well-crystallized sepiolite, as indicated by the characteristic narrow and intense diffraction peak, corresponding to the interlayer distance in the sepiolite structure. The other peaks in the same pattern belong to sepiolite.

All chemicals were obtained from Merck and Aldrich, and they were of analytical grade. All water used was of Milli-Q quality or doubly distilled.

2.3. Experimental procedure

Sorption kinetic experiments were carried out using mechanic stirrer. All of the dye solutions were prepared with ultra-pure water. Kinetic experiments were carried out by agitating 2 L of dye solution of initial concentration 2×10^{-3} mol/L at a constant agitation speed of 400 rpm, 1×10^{-3} mol/L ionic strength (NaCl), 298 K, and pH 8.5. Agitation was made for 60 min [29], which is more than sufficient time to reach equilibrium at a constant agitation speed of 400 rpm. Preliminary experiments had shown that the effect of the separation time on the adsorbed amount of dye was negligible. The initial tested concentrations of MR-GRL solution were 1.5×10^{-3}, 2.0×10^{-3}, and 2.5×10^{-3} mol/L. The effect of pH was analyzed in the pH range from 5 to 10. The pH profiles of sepiolite in a 0.3 wt.% suspension as a function of time is presented in Ref. [30] at an initial pH of neutral, acidic, and basic media. When the initial pH is adjusted to 10, after sepiolite addition, the suspension pH comes down to 9.05 in 24 h. When sepiolite is added to distilled water at pH 7.13 (in water), the suspension pH rises and then remains almost constant upon reaching the equilibrium pH of 8.55 after 24 h [30]. Thus, pH was chosen as 8.5 for all experiments because it is difficult to keep constant at pH 10 except for experiments of effect of pH. The pH was adjusted using 0.1 N NaOH and 0.1 N HCl solutions by using an Orion 920A pH meter with a combined pH electrode. pH meter was standardized with NBS buffers before every measurement. The effect of ionic strength was investigated at 0.001–0.100 mol/L NaCl salt concentrations. The experiments carried out at 288, 298, 308, and 318 K were set with a thermostat. Two milliliters of samples was taken from reactor in various times. The samples were then centrifuged for 15 min at 5,000 rpm and the left out concentration in the supernatant solution was analyzed using Cary 1E UV–vis spectrophotometer, (Varian) by monitoring the absorbance changes at a wavelength of maximum absorbance (531 nm). Each experimental run continued until no significant change in the dye concentration was measured. Calibration curves were plotted absorbance against concentration of the dye solution. The adsorbed amount of dye at any time *t*, q_t, was calculated from the mass balance equation [29,31].

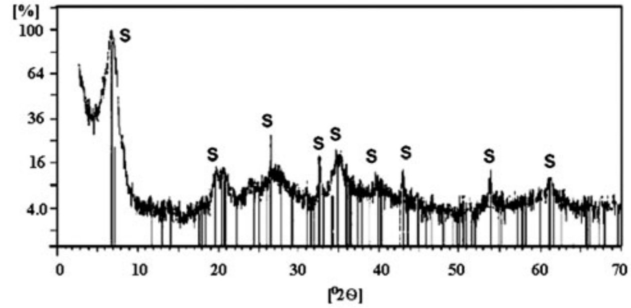

Fig. 3. XRD pattern of sepiolite.

Table 2
Some physicochemical properties of sepiolite used in this study

CEC (meq/100 g)	Particle diameter (μm)	pH of 3% aqueous solution	Density (g mL^{-1})	Specific surface area (m^2 g^{-1})	Porosity (%)	Color
23.0	−75.0	7.9–8.4	2.45	355	50.5	White

3. Results and discussion

3.1. Adsorption rate

In order to characterize the adsorption process of the dye on sepiolite, in this section, we have discussed the effect of factors such as contact time, stirring speed, initial dye concentration, initial solution pH, ionic strength, and solution temperature on the removal rate of cationic dye onto sepiolite from aqueous solution.

3.1.1. Effect of contact and equilibrium times and initial dye concentration

The adsorption of MR-GRL dye on sepiolite at different initial concentrations and stirring speed of 400 rpm was studied as a function of contact time in order to determine the equilibrium time. Fig. 4 shows time effect of the adsorption equilibrium of MR-GRL onto sepiolite. The removal of dye was rapid in the initial contact time and gradually decreased with equilibrium. Due to the presence of active sites on the sepiolite surface, the adsorption was observed rapidly during the first 20 min, then sorption occurred was less because of occupancy of these sites. The initial concentration provides an important driving force to overcome mass transfer resistances of all molecules between the aqueous and solid phases [31,32]. Fig. 4 shows the amount of dye adsorbed vs. time at different initial dye concentrations. Figure showed that the amount of dye adsorbed gets increased from 2.12×10^{-4} to 3.93×10^{-4} mol g^{-1} for an increase in initial dye concentration from 1.5×10^{-3} to 2.5×10^{-3} mol/L.

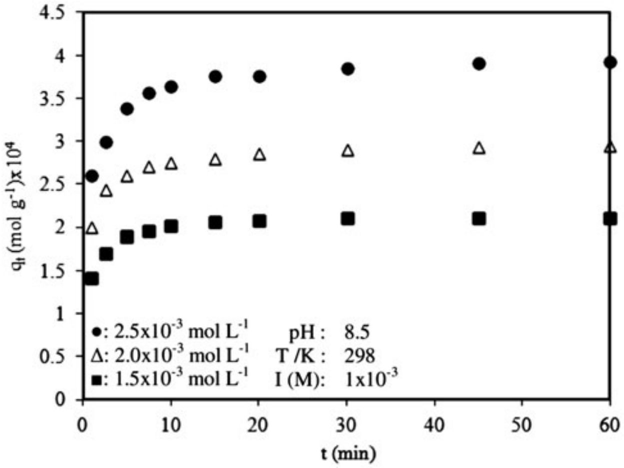

Fig. 4. The effect of initial dye concentration for the adsorption rate of MR-GRL on sepiolite.

3.1.2. Effect of stirring speed

The effect of stirring speed on removal rate of MR-GRL with sepiolite was investigated at different stirring speeds at 200, 400, and 600 rpm. Stirring speed is an important parameter in adsorption phenomena, influencing the distribution of the solute in the bulk solution and the formation of the external boundary film. Table 3 shows the sorption of MR-GRL by sepiolite adsorbent at different stirring speed, ranging from 200 to 600 rpm using a contact time of 60 min. The amount of adsorbed dye at equilibrium sorption capacity, increased with increasing stirring speed. This can be explained that increasing agitation speed reduced the film boundary layer surrounding

Table 3
Kinetic data calculated for adsorption of MR-GRL on sepiolite

Parameters							Second-order kinetic models				
T (K)	Conc. (mol/L) × 10^3	pH	Stirring speed (rpm)	[I] (mol/L)	q_e (cal) (mol g^{-1}) × 10^4	q_e (exp.) (mol g^{-1}) × 10^4	k_2 (g mol^{-1} min^{-1})	k_L (L g min^{-1} m^{-2}) × 10^3	R^2	h (mol min^{-1} g^{-1}) × 10^4	$t_{1/2}$ (s)
288	2	8.5	400	0.001	2.88	2.84	5655.7	1.645	1.000	4.570	37.33
308	2	8.5	400	0.001	3.40	3.39	6320.2	2.615	0.999	7.270	27.99
318	2	8.5	400	0.001	3.61	3.67	7558.8	3.550	0.999	10.150	21.65
298	2	10.0	400	0.001	3.22	3.16	2887.2	1.080	0.999	2.880	65.76
298	2	8.5	400	0.001	2.97	2.95	4626.4	1.470	0.999	4.020	43.96
298	2	5.0	400	0.001	2.34	2.31	6313.4	1.245	0.999	3.370	41.08
298	2	8.5	200	0.001	2.80	2.78	6663.8	1.880	1.000	5.150	32.38
298	2	8.5	600	0.001	3.05	3.02	4470.6	1.500	9.999	4.090	44.33
298	1.5	8.5	400	0.001	2.14	2.12	8322.5	1.830	1.000	3.715	34.12
298	2.5	8.5	400	0.001	3.97	3.93	3024.8	1.375	0.999	4.671	50.47
298	2	8.5	400	0.010	2.86	2.83	4188.9	1.235	0.999	3.350	50.60
298	2	8.5	400	0.100	2.74	2.67	1916.5	0.520	0.999	1.370	117.2

particles, thus increasing the external film transfer coefficient, and hence the adsorption capacity. This result is surprising since the agitation speed can change the kinetics, not the equilibrium capacity [32]. McKay [33] reported that the rate of dye removal was influenced by the degree of agitation and the uptake increased with stirring rate. The degree of agitation reduced the boundary layer resistance and increased the mobility of the system. An agitation speed of 400 rpm was chosen for further experiments.

3.1.3. Effect of solution pH

From Table 3, it was observed that the solution pH affects the amount of dye adsorbed. The dye uptake was found to increase with increasing pH and it increases from 2.31×10^{-4} to $3.16 \times 10^{-4}\,\mathrm{mol\,g^{-1}}$ for a pH from 5 to 10. Data in Table 3 demonstrate that the adsorption increases with increasing pH because of the electrostatic attraction between the chromophore groups of dye and the negatively charged sepiolite surface. The higher adsorption of MR-GRL on sepiolite at high pH may result from the neutralization of the negative sites on the surface of sepiolite. We had previously shown that sepiolite had an isoelectric point at pH 6.6 and exhibited positive zeta potential values at pH lesser than 6.6 and negative zeta potential values at pH higher than 6.6 [30]. When pH increased from 5 to 10, the number of active sites on sepiolite increased, as seen in Eq. (1).

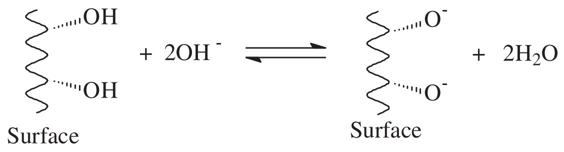

(1)

When the surface of sepiolite becomes negatively charged at high pH, electrostatic forces of the positively charged MR-GRL cations enhance the attraction [34] and this situation is summarized in Eq. (2).

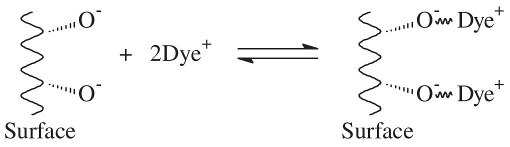

(2)

3.1.4. Effect of ionic strength

As seen in Table 3, the presence of inorganic salt has significantly influenced the adsorption rate of MR-GRL. For the adsorption of MR-GRL by sepiolite, the adsorption was found to decrease with increasing ionic strength. Since the salt screens the surface through competing adsorption of opposite of the oxide surface and the dye molecules, the adsorbed amount will decrease with increase of NaCl concentration [34].

3.1.5. Effect of temperature

Table 3 shows the adsorption kinetics of MR-GRL at 288, 298, 308, and 318 K by plotting adsorption capacity, q_t, vs. time at the initial dye concentration of 2×10^{-3} mol/L. Increasing the temperature increases the rate of diffusion of the adsorbate molecules across the external boundary layer and in the internal pores of the adsorbent particle, owing to the decrease in the viscosity of the solution [29,31]. In addition, changing the temperature will change the equilibrium capacity of the adsorbent for a particular adsorbate [29,34]. When the temperature was increased, the removal of dye by adsorption onto sepiolite increased from 2.84×10^{-4} to $3.67 \times 10^{-4}\,\mathrm{mol\,g^{-1}}$ by increasing the temperature of the solution from 288 to 318 K, indicating that the process is endothermic.

3.2. Adsorption kinetics

In order to examine the controlling mechanism of sorption process, several kinetic models were used to test the experimental data.

3.2.1. Pseudo first- and second-order equations

The pseudo-first-order equation is generally expressed as follows (Eq. (3)) [35]:

$$\ln(q_e - q_t) = \ln q_e - k_1 t \tag{3}$$

where q_e and q_t are the amounts of dye ions adsorbed at equilibrium and time t ($\mathrm{mol\,g^{-1}}$), respectively, and k_1 is the rate constant of pseudo-first-order adsorption ($\mathrm{min^{-1}}$).

The pseudo-second-order equation is expressed by (Eq. (4)) [35]:

$$\frac{t}{q_t} = \frac{1}{k_2 q_e^2} + \frac{1}{q_e} t \tag{4}$$

where q_e is the amount of dye ions adsorbed at equilibrium ($\mathrm{mol\,g^{-1}}$) and k_2 is the equilibrium rate constant of pseudo-second-order sorption ($\mathrm{g\,mol^{-1}\,min^{-1}}$).

The half-adsorption time of the dye ions, $t_{1/2}$, is expressed in the following Eq. (5):

$$t_{1/2} = \frac{1}{k_2 q_e} \tag{5}$$

The initial adsorption rate, h (mol g^{-1} min^{-1}) is expressed by (Eq. (6)):

$$h = k_2 q_e^2 \tag{6}$$

The values k_2, q_e, $t_{1/2}$, and h are given in Table 3. As shown in Table 3, experimental data can be explained by pseudo-second-order kinetic equation.

3.2.2. The diffusion coefficients, intraparticle diffusion equation, and mass transfer

The diffusion coefficients were calculated under various conditions for the adsorption of MR-GRL on sepiolite surface by employing the following Eq. (7):

$$t^{1/2} = \frac{0.030 r_0^2}{D} \tag{7}$$

where D is the diffusion coefficient with the unit cm^2/s; $t^{1/2}$ is the time (s) for half adsorption, and r_0 is the radius of the adsorbent particle in cm. The value of r_0 was calculated as 18.75×10^{-4} cm for sepiolite sample. Table 4 shows the diffusion coefficients calculated for adsorption of MR-GRL on sepiolite from aqueous solutions. We found that the diffusion coefficients changed in the range from 2.85×10^{-9} to 8.65×10^{-9} cm^2/s under various conditions.

The initial rate of the intraparticle diffusion is in the following Eq. (8) [29,35]:

$$q_t = k_{\text{int}} t^{1/2} + C \tag{8}$$

where k_{int} is the intraparticle diffusion rate constant (mg g^{-1} min$^{-1/2}$) and is given in Table 4.

Fig. 5 shows the plot q_t against to $t^{0.5}$ for MR-GRL adsorption onto sepiolite surface. Fig. 5 shows that the sorption process tends to be followed by two phases. The calculated intraparticle diffusion coefficients, $k_{\text{int},1}$ and $k_{\text{int},2}$ values at different conditions are shown in Table 4. Since $k_{\text{int},1}$ values for first part of plot are high, this step is not rate-limiting step. The slope of second linear portion of the plot has been defined as the intraparticle diffusion parameter $k_{\text{int},2}$ (mol/(g min$^{0.5}$)) [35,36].

For mass transfer, a linear graphical relation between $\ln[(C_t/C_0) - 1/(1 + mK)]$ vs. t was not obtained (equation from Ref. [30]). The values of regression coefficient calculated from mass transfer and intraparticle diffusion equations are given in Table 4.

3.3. Thermodynamic parameters

The second-order rate constants are used to estimate the activation energy of the MR-GRL adsorption on sepiolite using Arrhenius equation. The slope of plot of $\ln k_2$ vs. $1/T$ is used to evaluate E_a, which was found to be 22.69 kJ/mol. Low activation energies (5–40 kJ/mol) are characteristics for physisorption, while higher activation energies (40–800 kJ/mol)

Table 4
Adsorption mechanism and diffusion coefficients of MR-GRL on sepiolite

Parameters					Mechanism of adsorption					
					Mass transfer	Intraparticle diffusion				
T (K)	Conc. (mol/L) × 10^3	pH	Stirring speed (rpm)	[I] (mol/L)	R^2	$k_{\text{int},1} \times 10^5$ (mol g^{-1} min$^{-1/2}$)	$R_1{}^2$	$k_{\text{int},2} \times 10^6$ (mol g^{-1} min$^{-1/2}$)	$R_2{}^2$	D (cm^2 s^{-1}) × 10^9
288	2	8.5	400	0.001	0.533	3.56	0.981	2.94	0.736	5.021
308	2	8.5	400	0.001	0.731	3.89	0.921	3.89	0.834	6.698
318	2	8.5	400	0.001	0.824	3.97	0.981	3.97	0.928	8.657
298	2	10	400	0.001	0.652	4.17	0.962	7.00	0.856	2.851
298	2	8.5	400	0.001	0.726	3.87	0.902	4.36	0.926	4.265
298	2	5.0	400	0.001	0.887	3.35	0.855	2.90	0.884	4.563
298	2	8.5	200	0.001	0.755	3.60	0.923	2.68	0.859	5.789
298	2	8.5	600	0.001	0.622	3.69	0.890	4.55	0.928	4.228
298	1.5	8.5	400	0.001	0.578	3.14	0.955	1.81	0.775	5.495
298	2.5	8.5	400	0.001	0.618	5.60	0.987	6.02	0.911	3.715
298	2	8.5	400	0.010	0.805	3.05	0.996	4.26	0.909	3.700
298	2	8.5	400	0.100	0.624	3.69	0.953	9.44	0.923	1.600

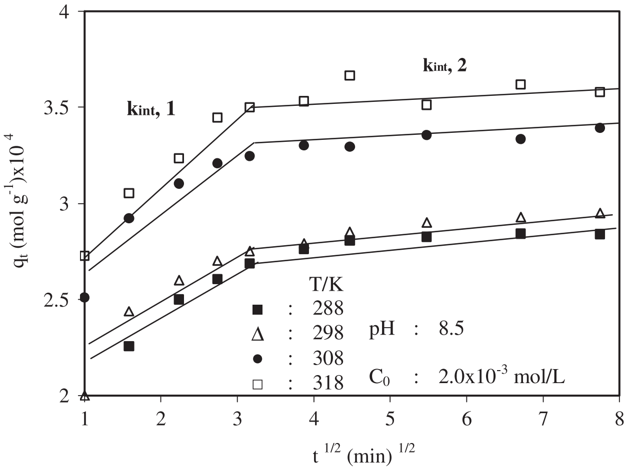

Fig. 5. Intraparticle diffusion plots for different temperatures.

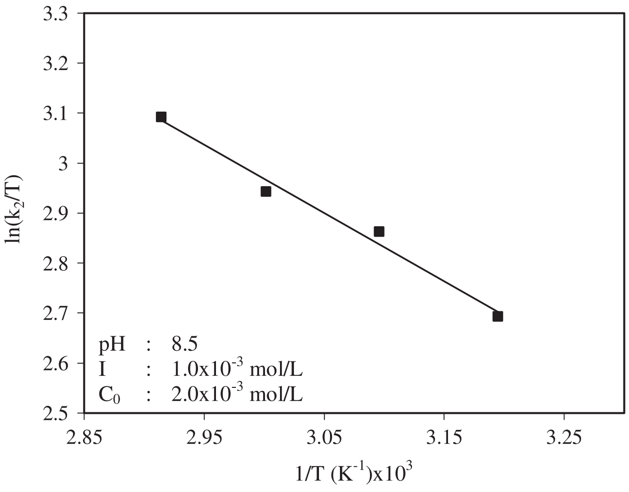

Fig. 6. Plot of ln (k_2/T) vs. $1/T$ for adsorption of MR-GRL on sepiolite.

suggest chemisorption [29,31]. The result obtained for the adsorption of MR-GRL onto sepiolite indicates that the adsorption has a potential barrier. Therefore, the thermodynamic activation parameters of the process such as enthalpy ΔH^*, entropy ΔS^*, and free energy ΔG^* were determined using the Eyring Eq. (9) [37]:

$$\ln\left(\frac{k_2}{T}\right) = \ln\left(\frac{k_B}{h}\right) + \frac{\Delta S^*}{R_g} - \frac{\Delta H}{R_g T} \tag{9}$$

where k_B is the Boltzmann constant (1.3807×10^{-23} J/K) and h is the Planck constant (6.6261×10^{-34} J s). Fig. 6 shows the plot of ln (k_2/T) against $1/T$. The result obtained for the change of Gibbs energy is +66.17 kJ/mol at 298 K. The value of the standard enthalpy change (19.92 kJ/mol) indicates that the adsorption is physical in nature involving weak forces of attraction and is also endothermic. At the same time, the low value of ΔH^* implies that the bonding between the adsorbate molecules and the adsorbent surface was loose [37]. The negative standard entropy change (ΔS^*) value (−147.6 J/(K mol)) corresponds to a decrease in the degree of freedom of the adsorbed species. Due to the adsorption process, the adsorbate molecules have a more regular structure. The system is tending to decrease in entropy. Furthermore, the negative values of entropy obtained for both the systems reveal that the internal structure of the sepiolite do not go through any significant change during the adsorption of the dye [38]. The ΔS^* and ΔH^* values are calculated as negative and positive, respectively. In these conditions, the free Gibbs energy cannot be negative from the formula of $\Delta G^* = \Delta H^* - T\,\Delta S^*$. This conclusion does not mean that the event itself but indicates that the active force for adsorption is electrostatic interaction between clay (negative surface) and dye (positive charge).

4. Conclusions

The present study shows that the sepiolite can be used as an adsorbent for the removal of MR-GRL from its aqueous solutions. The amount of dye uptake (mol g^{-1}) was found to increase with increase in contact time, initial dye concentration, stirring speed, pH, and solution temperature, and found to decrease with increase in ionic strength. The results demonstrate a significant linear relationship between adsorbed MR-GRL, t/q_t, and t in this study with high correlation coefficients. This suggests that the adsorption system is compatible with the second-order kinetic model. The dye uptake process was found to be controlled by intraparticle diffusion. Thermodynamic activation parameter shows that the process is endothermic. Sepiolite has a high potential to adsorb cationic dyes from aqueous solutions. Therefore, it can be effectively used as an adsorbent for the removal of this dye from wastewaters.

References

[1] M.S. Chiou, P. Ho, H.Y. Li, Adsorption of anionic dyes in acid solutions using chemically cross-linked chitosan beads, Dyes Pigm. 60(1) (2004) 69–84.
[2] K.P. Singh, D. Mohan, S. Sinha, G.S. Tandon, D. Ghosh, Colour removal from wastewater using low cost activated carbon derived from agricultural waste material, Ind. Eng. Chem. Res. 42 (2003) 1965–1976.
[3] I.M. Banat, P. Nigam, D. Singh, R. Marchant, Microbial decolourisation of textile-dye-containing effluents: A review, Bioresour. Technol. 58 (1996) 217–227.

[4] K.K.H. Choy, G. McKay, J.F. Porter, Sorption of acid dyes from effluents using activated carbon, Resour. Conserv. Recycl. 27 (1999) 57–71.

[5] M. Bülow, A. Micke, Determination of transport coefficients in microporous solids, Adsorption 1 (1995) 29–48.

[6] H.D. Do, D.D. Do, I. Prasetyo, Surface diffusion and adsorption of hydrocarbons in activated carbon, AIChE J. 47 (2001) 2512–2525.

[7] Y.S. Ho, Review of second-order models for adsorption systems, J. Hazard. Mater. 136 (2006) 681.

[8] M. Basibuyuk, C.F. Forster, An examination of the adsorption characteristics of a basic dye (Maxilon Red BL-N) on to live activated sludge system, Process Biochem. 38 (2003) 1311–1316.

[9] S. Wang, H. Li, Dye adsorption on unburned carbon: kinetics and equilibrium, J. Hazard Mater. 126 (2005) 71–77.

[10] G. McKay, M.S. Otterburn, A.G. Sweeney, The removal of colour from effluent using various adsorbents—III. Silica: Rate processes, Water Res. 14 (1980) 15–20.

[11] C.C. Wang, L.C. Juang, T.C. Hsu, C.K. Lee, J.F. Lee, F.C. Huang, Adsorption of basic dyes onto montmorillonite, J. Colloid Interface Sci. 273 (2004) 80–86.

[12] J. Mittal, V. Thakur, A. Mittal, Batch removal of hazardous azo dye Bismark Brown R using waste material hen feather, Ecol. Eng. 60 (2013) 249–253.

[13] A. Mittal, V. Thakur, V. Gajbe, Adsorptive removal of toxic azo dye Amido Black 10B by hen feather, Environ. Sci. Pollut. Res. 20 (2013) 260–269.

[14] A. Mittal, V. Thakur, J. Mittal, H. Vardhan, Process development for the removal of hazardous anionic azo dye Congo Red from wastewater by using hen feather as potential adsorbent, Desalin. Water Treat. 52 (2014) 227–237.

[15] A. Mittal, J. Mittal, L. Kurup, Utilization of Hen Feathers for the adsorption of Indigo Carmine from simulated effluent, J. Environ. Prot. Sci. 1 (2007) 92–100.

[16] A. Mittal, D. Jhare, J. Mittal, Adsorption of hazardous dye Eosin Yellow from aqueous solution onto waste material de-oiled soya: Isotherm, kinetics and bulk removal, J. Mol. Liq. 179 (2013) 133–140.

[17] A. Mittal, L. Kurup, Column operations for the removal and recovery of a hazardous dye 'acid red – 27' from aqueous solutions, using waste materials – bottom ash and de-oiled soya, Ecol. Environ. Conserv. 12(2) (2006) 181–186.

[18] H. Daraei, A. Mittal, M. Noorisepehr, F. Daraei, Kinetic and equilibrium studies of adsorptive removal of phenol onto eggshell waste, Environ. Sci. Pollut. Res. 20 (2013) 4603–4611.

[19] H. Daraei, A. Mittal, J. Mittal, H. Kamali, Optimization of Cr(VI) removal onto biosorbent eggshell membrane: Experimental & theoretical approaches, Desalin. Water Treat. (2013) 1–9. doi: 10.1080/19443994.2013.787374.

[20] H. Daraei, A. Mittal, M. Noorisepehr, J. Mittal, Separation of chromium from water samples using eggshell powder as a low-cost sorbent: kinetic and thermodynamic studies, Desalin. Water Treat. (2013) 1–7. doi: 10.1080/19443994.2013.837011.

[21] J. Mittal, D. Jhare, H. Vardhan, A. Mittal, Utilization of bottom ash as a low-cost sorbent for the removal and recovery of a toxic halogen containing dye Eosin Yellow, Desalin. Water Treat. (2013) 1–12. doi: 10.1080/19443994.2013.803265.

[22] S. Sadaf, H.N. Bhatti, Batch and fixed bed column studies for the removal of Indosol Yellow BG dye by peanut husk, J. Taiwan Inst. Chem. Eng. In Press. doi: 10.1016/j.jtice.2013.05.004.

[23] S. Sadaf, H.N. Bhatti, Evaluation of peanut husk as a novel, low cost biosorbent for the removal of Indosol Orange RSN dye from aqueous solutions: Batch and fixed bed studies, Clean Technnol. Environ. Policy. In Press. doi: 10.1007/s10098-013-0653-z.

[24] S. Noreen, H.N. Bhatti, S. Nausheen, S. Sadaf, M. Ashfaq, Batch and fixed bed adsorption study for the removal of Drimarine Black CL-B dye from aqueous solution using a lignocellulosic waste: A cost affective adsorbent, Ind. Crops Prod. 50 (2013) 568–579.

[25] A. Mittal, R. Jain, J. Mittal, M. Shrivastava, Adsorptive removal of hazardous dye Quinoline Yellow from waste water using coconut-husk as potential adsorbent, Fresenius Environ. Bull. 19(6) (2010) 1–9.

[26] J.L. Ahlrichs, J.C. Serna, J.M. Serratosa, Structural hydroxyls in sepiolite, Clays Clay Miner. 23 (1975) 119–124.

[27] G. Rytwo, D. Tropp, C. Serban, Adsorption of diquat, paraquat and methyl green on sepiolite: Experimental results and model calculations, Appl. Clay Sci. 20 (2002) 273–282.

[28] R.E. Grim, Clay Mineralogy, 2nd ed., McGraw-Hill, New York, NY, 1968.

[29] M. Alkan, Ö. Demirbaş, M. Doğan, Adsorption kinetics and thermodynamics of an anionic dye onto sepiolite, Microporous Mesoporous Mater. 101 (2007) 388–396.

[30] M. Alkan, Ö. Demirbaş, M. Doğan, Electrokinetic properties of sepiolite suspensions in different electrolyte media, J. Colloid Interface Sci. 281 (2005) 240–248.

[31] M. Doğan, M. Alkan, Ö. Demirbaş, Y. Özdemir, C. Özmetin, Adsorption kinetics of Maxilon Blue GRL onto sepiolite from aqueous solutions, Chem. Eng. J. 124 (2006) 89–101.

[32] G. Crini, H.N. Peindy, F. Gimbert, C. Robert, Removal of C.I. Basic Green 4 (Malachite Green) from aqueous solutions by adsorption using cyclodextrin based adsorbent: Kinetic and equilibrium studies, Sep. Purif. Technol. 53 (2007) 97–110.

[33] G. McKay, Adsorption of dyestuffs from aqueous solutions with activated carbon I: Equilibrium and batch contact-time studies, J. Chem. Technol. Biotechnol. 32 (1982) 759–772.

[34] N. Tekin, Ö. Demirbaş, M. Alkan, Adsorption of cationic polyacrylamide onto kaolinite, Microporous Mesoporous Mater. 85 (2005) 340–350.

[35] Y.S. Ho, G. McKay, Pseudo-second order model for sorption processes, Process Biochem. 34 (1999) 451–465.

[36] N. Kannan, M. Sundaram, Kinetics and mechanism of removal of methylene blue by adsorption on various carbons – a comparative study, Dyes Pigm. 51 (2001) 25–40.

[37] K.J. Laidler, J.M. Meiser, Physical Chemistry, Houghton Mifflin, New York, NY, 1999.

[38] V.K. Gupta, A. Mittal, D. Jhare, J. Mittal, Batch and bulk removal of hazardous colouring agent Rose Bengal by adsorption techniques using bottom ash as adsorbent, RSC Adv. 2 (2012) 8381–8389.